

1
2
3
4
5
6
7
8
9
10
11
12
13
14
15
16
17
18
19
20
21
22
23
24

High and Low Frequency 11-year Solar Cycle Signatures in the Southern Hemispheric Winter and Spring

Hua Lu^{1,a}, Martin J. Jarvis¹, Lesley J. Gray², Mark P. Baldwin³

Prepared for **Quarterly Journal of the Royal Meteorological Society**

^a Corresponding author.

¹ H. Lu and M. J. Jarvis, British Antarctic Survey, High Cross, Madingley Road, Cambridge CB3 0ET, England, UK.
(email: hl@bas.ac.uk; mjja@bas.ac.uk)

² L. J. Gray, NCAS-Climate, Department of Oceanic, Atmospheric and Planetary Physics, Oxford University, Oxford, OX1 3PU, UK. (email: lesley@atm.ox.ac.uk)

³ M. P. Baldwin, Northwest Research Associates, 4118, 148th Ave, Redmond, WA 98052, USA. (email: mark@nwra.com)

25

26 **Abstract:** We have studied the characterization of the 11-yr SC signals in the Southern Hemisphere
27 (SH) during the winter and spring using ECMWF daily and monthly data from 1979 to 2009. By
28 separating the response into high (< 6 months) and low (>36 months) frequency domains, we have
29 found spatially different 11-yr SC signals exist for high and low frequency domains. In the stratosphere,
30 the high and low frequency responses tend to enhance each other near the equator and subtropics while
31 they oppose one another at high latitudes. The high frequency response is marked by a strengthened
32 stratospheric jet during winter and the response is not static but tracks with the centre of the polar
33 vortex. In the lower stratosphere, the positive response of temperature to the 11-yr SC is dominated by
34 its low frequency component, which extends from the North Pole to the South Pole. The low frequency
35 tropospheric response is latitudinally symmetric about the equator and consistent with the modeled
36 responses to temperature perturbation in the lower stratosphere. The signals are found to be sensitive to
37 contamination from the 2002 sudden stratospheric warming event and major volcanic eruptions but the
38 general spatial pattern of the responses remain similar. A significant projection of the 11-yr SC onto the
39 SAM can only be detected in the stratosphere and in the high frequency component. The signature is
40 marked by a strengthening of the stratospheric SAM during winter and a weakening of the SAM in the
41 uppermost stratosphere during spring.

42

43

44

45

46 **1. Introduction**

47 Studies have shown that changes associated with the 11-year solar cycle (SC) have detectable
48 effects on the stratospheric and tropospheric circulation (*e.g.* Gleisner and Thejll 2003; Haigh 2003;
49 Coughlin and Tung 2004; Hood 2004; Salby and Callaghan 2006; Lu *et al.* 2007; van Loon *et al.* 2007).
50 The 11-yr SC signature in stratospheric temperature is characterized by positive correlation at low
51 latitudes with a vertical double-peaked structure, one in the lower stratosphere and another in the upper
52 stratosphere (Crooks and Gray 2005; Keckhut *et al.* 2005; Claud *et al.* 2008; Frame and Gray 2010;
53 Gray *et al.* 2010). In zonal-mean zonal wind, it is marked by a strengthening of the subtropical jet in the
54 upper stratosphere and a poleward and downward movement of westerly anomalies (Kuroda and Kodera
55 2002; Kodera *et al.* 2003; Gray *et al.* 2004; Matthes *et al.* 2004; ; Gray *et al.* 2010).

56 As the total solar irradiance varies by only $\sim 0.1\%$ over an 11-year solar cycle (11-yr SC), it has
57 been suggested that larger variations of solar ultra violet (UV) radiation ($\sim 5\text{-}8\%$ over an 11-yr SC) and
58 its absorption by stratospheric ozone could provide a detectable solar link to variation of the global
59 circulation (Haigh 1994; 2003). Thermal structure change caused by the associated heating in the upper
60 stratosphere may lead to a modulation of the stratospheric polar vortex and cause a dynamical feedback
61 in the lower stratosphere (Kodera and Kuroda 2002). The enhanced equatorial heating due to solar UV-
62 ozone interaction results in anomalously stronger westerlies in the upper stratosphere/lower mesosphere,
63 in thermal wind balance with an enhanced pole-to-equator temperature gradient. The stronger westerlies
64 may deflect planetary waves poleward and cause a further strengthening of the polar vortex (Kodera *et*
65 *al.* 2003). The solar UV induced wind anomalies move poleward and downward as the winter
66 progresses (Kodera and Kuroda 2002; Kodera *et al.* 2003; Matthes *et al.* 2004).

67 Perturbation of the stratosphere by UV radiation variations followed by downward propagation of
68 the resulting circulation anomalies to the surface has been proposed to explain the observed tropospheric
69 solar signals (Haigh *et al.* 2005; Hameed and Lee 2005; Matthes *et al.* 2006). Changes to the winter
70 stratospheric polar vortex may influence the underlying tropospheric circulation. In addition, idealized

71 model simulations have suggested that a solar modulation of the equatorial lower stratosphere, which
72 affects the equator-to-pole temperature gradient may also modulate the synoptic scale wave activity
73 (Haigh and Blackburn 2006; Simpson *et al.* 2009). GCMs studies also suggest that solar UV induced
74 change in the Brewer Dobson (BD) circulation in the upper stratosphere can cause a suppression of
75 tropical convection during solar maximum (Kodera 2004; Kodera and Shibata 2006; Matthes *et al.*
76 2006). One thing in common with the above proposed mechanisms is that they all involve a
77 stratospheric influence on the tropospheric circulation and they are consequently referred to as “top-
78 down’ mechanisms (Gray *et al.* 2010).

79 Another mechanism of solar influence over an 11-year cycle is through air-sea-radiative coupling
80 at the ocean surface in the tropics whereby the spatial asymmetries of solar forcing, induced by cloud
81 distributions, result in greater evaporation in the subtropics and consequent moisture transport into the
82 tropical convergence zones (Meehl *et al.* 2003). Higher solar forcing may cause stronger upward motion
83 in the winter hemispheric subtropics and enhanced downward motion in the summer hemisphere
84 subtropics (van Loon *et al.* 2004; Meehl *et al.* 2008). As it involves near surface processes and because
85 significant responses have been detected in models without a stratosphere, it is consequently referred to
86 as the “bottom-up” mechanism (Gray *et al.* 2010). For a recent review of all proposed mechanisms of
87 solar influence on the climate, see Gray *et al.* (2010).

88 It is possible to study each individual mechanism separately using models but it is very difficult to
89 separate the responses associated with different mechanisms using observational data. This presents a
90 substantial challenge to interpret the solar signals of different origin/cause based on the observational
91 signature. Proposed mechanisms involve fast processes such as wave mean flow interaction and/or slow
92 processes such as temperature change induced by redistribution of ozone in the lower stratosphere and
93 differential ocean heating. For instance, the wave driven dynamic response to the 11-yr SC tends to
94 change on sub-monthly time-scales (*e.g.* Kodera 2004; Matthes *et al.* 2006; Lu *et al.* 2009) while the
95 radiative response is more likely to be static over an extended period, especially in the lower
96 stratosphere, and hence can be detected in the annual mean (*e.g.* Keckhut *et al.* 2005; Claud *et al.* 2008;

97 Frame and Gray 2010). It is natural to think that the responses associated with fast processes may show
98 signals with a high frequency component within the atmospheric data while processes with slow
99 responses may be detected better in the low frequency domain.

100 In an attempt to refine the traditional way of analyzing the atmospheric response to the 11-yr SC,
101 here we separate the atmospheric data into high and low frequency domains, so that we are able to
102 examine the characterization of the solar signal in terms of fast *versus* slow processes, direct *versus*
103 indirect effects, radiative *versus* dynamic responses and their possible links to “top-down” and/or
104 “bottom-up” mechanisms. We focus on the Southern Hemispheric (SH) winter and spring where the
105 polar vortex is stronger and longer-lived than its NH counterpart due to weaker planetary wave forcing.
106 This implies that radiative interaction is likely to play a relatively larger role in the SH winter than in the
107 Northern Hemispheric (NH) winter, and the solar signals in the SH have been found to be different to
108 those in the NH (Labitzke 2002; Salby and Callaghan 2006). The dynamically “calm” SH winter may in
109 fact present a better environment to differentiate high and low frequency responses as the signals are
110 less likely to be affected by transient events such as stratospheric Sudden Warmings (SSWs). For
111 example, the modeling study of Cnossen *et al.* (2011) showed that the high latitude stratospheric and
112 tropospheric responses differ significantly for the SSW condition and non-SSW conditions. By
113 focusing on the SH winter and spring, we can understand more how the 11-yr SC signal behaves under
114 non-SSW conditions.

115 Though our main focus is on detecting high and low frequency solar responses in the Earth’s
116 atmospheric temperature and zonal wind and to study how those signals might be linked to previously
117 proposed mechanisms, we also study whether or not the 11-yr SC may project onto the Southern
118 Annular Model (SAM) more clearly if the data are separated into high and low frequency components.
119 Because the stratospheric effects on the troposphere may be realized through the SAM and the coupling
120 depends primarily on wave activity (Thompson *et al.* 2005; Limpasuvan and Hartmann 2000), it is
121 expected that the high frequency component plays a more important role than the low frequency
122 component. In this study, we shall check if it is also the case for the 11-yr SC signal on the SAM.

123 Previous studies have shown that the large-scale structure of the late winter and spring SAM is
124 modulated by the 11-yr SC (*e.g.* Kuroda and Kodera 2004, 2005; Kuroda *et al.* 2007; Kurada and
125 Yamazaki 2010). These authors have shown that the 11-yr SC modulates the spatial structure of the
126 SAM from October through to December. In solar maximum years, the solar influence on the SAM
127 extends vertically from the surface to the upper stratosphere while it is capped within the troposphere
128 during solar minimum years. Using a coupled chemistry-climate model, Kuroda and Shibata (2005)
129 found that increases in solar UV radiation led to a stronger signal of the SAM in the Antarctic
130 stratosphere than during low UV runs. Unlike those previous studies, our main focus here is detecting
131 the 11-yr SC signals in the atmospheric variables including the SAM rather than the modulating effect
132 of the 11-yr SC on the SAM signature. More precisely, we do not study how the spatial extent of the
133 SAM signature in wind or temperature changes under high and low solar conditions. Instead, we study
134 how much of the interannual variability of the SAM may be directly linked to the 11-yr SC variation
135 and at what frequency and altitude such a linkage may be statistically significant.

136 The rather sparse observational network before the satellite era (*i.e.* pre- September 1978) in the
137 Southern Hemisphere (SH) limits the accuracy of the ERA-40 reanalysis before 1979. As a result, few
138 observational studies of the atmospheric response to the 11-yr SC have been undertaken for the SH
139 winter and spring. With a relatively short record length, it is important to consider the influence of other
140 major physical disturbances. Stratospheric sudden warmings (SSWs) have so far been recorded in the
141 SH on only one occasion, which was in 2002. Consequently in the 2002 winter and spring, the
142 stratospheric wind and temperature are distinctly anomalous to the other years (Charlton *et al.* 2005;
143 Scaife *et al.* 2005). In addition to the primary focus of this study, the dynamic features of 2002 will be
144 briefly discussed in the context of the atmospheric response to solar forcing. Also, the possible
145 contamination of results by the temporary warming associated with volcanic aerosols will also been
146 examined by comparing results after excluding and including two years of data following two major
147 eruptions (*i.e.* El Chichón in March 1982, and Pinatubo in June 1991). Due to the limited sample size,
148 the modulating effect of the equatorial Quasi-biennial Oscillation (QBO) will not be explicitly studied

149 here as statistical significance cannot be reliably established with any further sub-sampling, though the
150 possible effect of the QBO on the detected solar signals will be briefly discussed.

151 **2. Data and Methods**

152 Data used by this study are daily mean zonal winds and temperatures blended from the ECMWF
153 ERA-40 Reanalysis (January 1979 to August 2002) and ECMWF Operational analyses (September
154 2002 to December 2009), as employed by Frame and Gray (2010). The ERA-40 dataset was assimilated
155 using direct radiosonde and satellite measurements and has a horizontal resolution of 1.125° in both
156 latitude and longitude on 23 pressure levels from 1000 hPa to 1 hPa (Uppala *et al.* 2005). The ECMWF
157 Operational data were output from the ongoing analyses produced by the most recent ECMWF
158 Integrated Forecasting System (IFS) model. Data from September 2002 to the present day are available
159 on the same 1.125° grid but on 21 pressure levels (before 07/11/2007) and 25 pressure levels (since
160 07/11/2007). The ERA-40 and the Operational data sets share 21 of the pressure levels, the exceptions
161 being four levels in the lower troposphere (*i.e.* 600, 775, 900, and 950 hPa). For simplicity, only the data
162 for those 21 pressure levels are used here. Both ERA-40 and Operational datasets extend to 1 hPa (~50
163 km), thus allowing an examination of the solar signals throughout the stratosphere. While it is not ideal
164 to merge two datasets derived from different data assimilation models, we have done this here in order
165 to maximize the length of the data set, as needed for the study of 11-yr SC signals.

166 The daily data have not previously been used for this purpose; therefore this work is
167 complementary to earlier analyses by providing a more detailed temporal resolution on the timing of the
168 solar signals and their propagation pathways. Before the satellite era (*i.e.* before September 1978), the
169 scarcity of SH radiosonde measurements and lack of direct measurement at altitudes above 10 hPa result
170 in unreliable estimations in ERA-40, particularly in the upper stratosphere. To better capture solar
171 perturbation of the stratosphere by UV variations and the downward propagation of the resulting
172 circulation anomalies, only data from January 1979 onwards are used. The entire period of 1979-2009
173 covers 31 years and about three 11-yr SCs.

174 Daily observed 10.7-cm solar radio fluxes were obtained from the National Geophysical Data
175 Center (NGDC) website and are used as a proxy for the 11-yr SC. Their power spectrum shows that the
176 variability in the daily 10.7-cm solar radio fluxes is dominated by two frequency bands, one around 26-
177 28-days and another around 9.5-11.5 years. In order to focus on the 11-yr SC, a 365-day low-pass filter
178 was applied to the solar radio fluxes. The filtered daily time series is denoted as F_s hereafter and were
179 used in the analysis. Qualitatively similar results can be obtained if a running average window of 1-12
180 months is applied to the daily solar data. Noisier but qualitatively similar results can also be obtained by
181 using the raw daily fluxes. Similar to Lu *et al.* (2007; 2009), we use $\overline{F_s} < -0.25$ and $\overline{F_s} > 0.25$ to define
182 low solar (LS) and high solar (HS) activity when deriving composites where $\overline{F_s}$ stands for the
183 normalized values of F_s ; transition years where $|\overline{F_s}| \leq 0.25$ are excluded. Under this definition, 11 years
184 (*i.e.* 1979-1982, 1989-1992, and 1999-2001) were HS years and 15 years (*i.e.* 1984-1987, 1994-1998,
185 and 2004-2009) were LS years for June to October mean.

186 A possible projection of solar signal onto the Southern Annular Mode (SAM) is studied by using the
187 SAM index derived from two different sources. The first is the daily SAM index derived as the leading
188 empirical orthogonal function (EOF) of daily zonal-mean zonal wind over 20°–90°S, from the blended
189 ECMWF ERA-40 reanalysis and operational data for the same period. Details about this method can be
190 found in Baldwin and Thompson (2009). The second type of SAM index is the station-based SAM
191 index, which is estimated as a monthly mean difference between the mean sea level pressure anomaly at
192 six stations close to 40°S and six stations close to 65°S (Marshall 2003, available at
193 www.nercbas.ac.uk/icd/gjma/sam.html). By only using long-term stations and surface pressure
194 measurements, this index avoids the possible bias problems when combining the ERA-40 and ERA-
195 operational datasets. Thus, the principal advantages of the Marshall (2003) index are its simplicity and
196 temporal consistency across its entire time-span and between different seasons. As the station based
197 SAM extends back to 1957, it is used to test the robustness of the signals near the surface. For
198 simplicity, these two SAM indices are referred to hereinafter as daily ECMWF-SAM and monthly
199 Marshall-SAM, respectively.

200 The main diagnostic tools used are composite analysis and linear regression with standard Student
201 t -test being used to test their significance. The analyses were carried out for a range of frequency bands
202 where Chebyshev filters (Smith 1997) are used to separate one band of frequencies from another.
203 Chebyshev type II is used as high-pass filter while Chebyshev type I is used as low-pass filter. The main
204 criteria in designing the filters are a small (i.e. $< 0.5\%$) peak-to-peak ripple and stability for all
205 geographical locations. Through a large number of computational experiments, we found that a high-
206 pass filter with an order of 15-17 and peak-to-peak ripple of 2-5 dB in the normalized passband was
207 optimal for monthly data and an order of 3-5 was sufficient for daily data. For the low-pass and
208 bandpass filter, filter orders in the range of 4-9 for the monthly mean and 1-3 for daily data are
209 sufficient. In the sections below, a ripple magnitude of 2-dB is used throughout. Similar results can be
210 obtained if a Butterworth filter is used though higher order filters are required.

211 **3. Solar Signal during SH Winter and Spring**

212 **3.1 Winter and spring mean signals**

213 Figure 1 shows composite differences (HS-LS) of June-August averaged zonal-mean temperature
214 ($\Delta T_{\text{HS-LS}}$, 1st column) and zonal wind ($\Delta U_{\text{HS-LS}}$, 2nd column), in meridional-height cross section. When
215 the entire record is used ((a;e)), significant responses to the 11-yr SC are detected primarily in
216 temperature and in the stratosphere. In temperature, significant positive $\Delta T_{\text{HS-LS}}$ are found to extend
217 from 90°N to 40°S latitudinally and from 7hPa to 100 hPa vertically. Near the equator, $\Delta T_{\text{HS-LS}}$ is
218 statistically significant at a 95% confidence level only at ~70 hPa and not significant at other altitudes.
219 In the polar SH, $\Delta T_{\text{HS-LS}}$ displays an alternating vertical negative and positive pattern, which is most
220 likely to be an artifact of the dataset rather than a real response. Significant $\Delta U_{\text{HS-LS}}$ is found in the mid-
221 latitude stratosphere in the NH. In the SH, though $\Delta U_{\text{HS-LS}}$ is marked by westerly anomalies at 15-45°S
222 and easterly anomalies at poleward of 55°S, they are not significant at a 95% confidence level.

223 A similar response pattern can be obtained if selected anomalous data are excluded, *i.e.* 2002 major
224 SSW (b;f), the major volcanic eruptions (c;g) and both the major SSW and the volcanic eruptions,
225 although the magnitude and significance of the differences change slightly. Possible contaminations by

226 the major SSW and the volcanic eruptions can be viewed as enhancement or weakening of the solar
227 signals. When data from 2002 are excluded, the low-latitude temperature response is enhanced and the
228 westerly anomalies at 15-45°S become significant. When the years affected by the major volcanic
229 eruptions are excluded, the temperature response becomes weaker (< 0.3 K) in the lower stratosphere
230 and stronger (~ 0.5 K) in the upper stratosphere. Thus, the positive solar signature in lower-stratospheric
231 temperature is amplified by the bias of the eruptions of El Chichón and Mount Pinatubo. Almost no
232 significant signals can be found in the troposphere except for the westerly anomalies near the equator in
233 the SH.

234 **[[Insert Figure 1 here]]**

235 It has been suggested that the lack of statistically significant solar signals at 5-50 hPa in the tropics is
236 likely due to a contamination effect of the QBO (Smith and Matthes 2008). To examine such a
237 possibility in a simple manner, the same composite analysis is carried out at two distinct frequency
238 domains distinctly away from the typical period of the QBO (~ 28 months). Figure 2 shows the June-
239 August zonal-mean temperature (a;b;c) and zonal wind (d;e;f) responses to the 11-yr SC when a 6-
240 month high-pass filter (a;d), 36-month low-pass filter (b;e) and linearly detrend plus 36-month low-pass
241 filter are applied to the atmospheric data, respectively. Where a 6-month high-pass filter is applied to the
242 data, the primary feature of the temperature response to the 11-yr SC is positive $\Delta T_{\text{HS-LS}}$ in the
243 equatorial and subtropical stratosphere and at high latitude in the NH upper stratosphere. In the high
244 latitude SH, there are alternating positive and negative anomalies, but only the negative ones are
245 significant at the 0.05 level (*i.e.* a confidence level of 95% or above), implying a dominated cooling
246 effect in the region under HS condition. A small region near the equator in which a 95% confidence
247 level cannot be achieved is found at ~ 10 -20 hPa, though a positive temperature difference remains there.
248 The accompanying solar signals in zonal wind are marked by westerly anomalies up to 12 m/s in the SH
249 subtropical stratosphere extending downward from 1hPa to 70 hPa and 3 m/s in the NH subtropical
250 stratosphere extending downward from 1hPa to 20 hPa. Easterly anomalies are found in the high-
251 latitude upper stratosphere but are only significant in the NH at 55-75°S, 1-2hPa (see Figure 2(d)). A
252 similar pattern of solar response is obtained if the high-pass cutoff period is in the range of 3 to 12

253 months, and the magnitude and significance of the responses reduce when the cutoff period is either
254 smaller than 3 months or greater than 12 months. With a 36-month low-pass filter (see Figure 2b;e), the
255 temperature response is marked by a general positive ΔT_{HS-LS} in the stratosphere where a significant 11-
256 yr SC signal appears near the equator, in the subtropics and also in the polar region. The corresponding
257 response in the zonal wind is broadly symmetric about the equator. In the upper stratosphere, it is
258 characterized by statistically significant westerly anomalies in the subtropics and partly significant
259 easterly anomalies poleward of 60° . In the middle to lower stratosphere, it is marked by easterly
260 anomalies near the equator and in the region poleward of 60° and by westerly anomalies at mid-
261 latitudes. In the troposphere, it is marked by westerly anomalies near the equator and by easterly
262 anomalies near 30° and in the region poleward of 60° . The clearest vertical connection of the signals is
263 present in the westerly anomalies originating in the subtropical upper stratosphere. The spatial pattern
264 remains similar when the lower cutoff period is anywhere in the range of 12-36 months. However, the
265 equatorial-symmetric signal becomes noticeably stronger and clearer when the cutoff period is greater
266 than 28 months because the contamination of the QBO is suppressed.

267 It is known that there has been a steady decrease of the temperature in the stratosphere and increase
268 of the temperature in the troposphere over the last three decades and the diagnosis of the solar signal is
269 sensitive to the presence of trends in the data (Lu *et al.* 2007; Kodera *et al.* 2008; Frame *et al.* 2010). To
270 account for the effect of the long-term trends, the atmospheric data is first detrended linearly before
271 applying a 36-month low-pass filter (Figure 2c;f). The results of this show that the effects of removing
272 the linear trend give a generally weaker and less significant response in the stratosphere and an
273 enhanced response in the troposphere. In particular, at $30-50^\circ$ in both hemispheres, a significant positive
274 temperature response (~ 0.4 K) in the troposphere appears only when the long-term trend is removed.
275 Conversely, only marginal changes in zonal wind response are found to be associated with long-term
276 trend. There is an indication that the high and low frequency responses in tropospheric temperature are
277 of the opposite sign though the high frequency responses are hardly significant at a 95% confidence
278 level. More data are needed to confirm such a cancellation effect. Unlike temperature, the signature in
279 zonal wind is not sensitive to the long-term trends.

280 3.2 Seasonal progression of high frequency signals

281 It has been suggested that the temperature responses in the lower stratosphere are likely to be indirect
282 responses either through a modification of the Brewer-Dobson (BD) circulation, changes in ozone
283 transport or both (Kodera and Kuroda 2002; Hood 2004; Gray *et al.* 2009; Marsh and Garcia 2007;
284 Hood and Soukharev 2006; SPARC CCMVal report 2010). In this section, we focus on the temporal
285 evolution of the high frequency signal which helps the diagnosis of dynamical responses. We also show
286 how the high frequency signals in the upper stratosphere might contribute to those in the lower
287 stratospheric temperature, through a downward propagating mechanism which is likely to be associated
288 with changes in BD circulation. Daily data are used to demonstrate that solar UV forcing in the upper
289 stratosphere may be transferred dynamically through a downward and poleward movement of the
290 signals.

291 3.2.1 Signals in temperature

292 Figure 3 shows the monthly zonal-mean temperature (T_{clim}) for June to October (1st column) and
293 the corresponding 6-month high-pass filtered temperature differences $\Delta T_{\text{HS-LS}}$ (2nd and 3rd columns), all
294 displayed in meridional-height cross section with latitude extending from 30°N to 90°S. The
295 corresponding zonal wind signals are described in the next section. In June, a significant positive $\Delta T_{\text{HS-LS}}$
296 signal emerges in the equatorial and sub-tropical upper stratosphere (5-10hPa) and in the lower
297 stratosphere (70 hPa). The upper stratospheric signature enhances in July and latitudinally expands and
298 descends towards the lower stratosphere in August. Significant negative values of $\Delta T_{\text{HS-LS}}$ are found in
299 the high latitude SH in July and August. Such a response pattern in temperature suggests an enhanced
300 equator-to-pole temperature gradient in both the upper and lower stratosphere. The high latitude and
301 lower stratospheric tropical responses would be expected from a weakened BD circulation in solar
302 maximum years or from a strengthened BD circulation during solar minimum years. The temperature
303 responses both at low and high latitudes weaken in spring (September and October) and the high-
304 latitudinal negative signals are replaced by positive temperature responses.

305 **[[Insert Figure 3 here]]**

306 Figure 4 shows the daily running regression (in K per 100 solar unit) of zonal-mean temperature on
307 F_s averaged over 5°S to 5°N (a;c;e), and 55°S to 65°S (b;d;f), where data from 2002, 1982, 1983, 1991
308 and 1992 are excluded. In Figure 4(a;b), the regression is performed based on raw zonal-mean
309 temperatures at those two latitude bands and daily F_s . It shows that a downward descent of the positive
310 temperature anomalies with maximum magnitude of 3 K per 100 solar unit is found at ~2 hPa near the
311 equator in late June (Figure 4a). The signal descends to 20 hPa in late August. There is a weaker but
312 significant (*i.e.* at the confidence level of 95% or above) temperature response at 70 hPa for the same
313 period which does not show any direct vertical connection with that originating in the equatorial upper
314 stratosphere. A negative temperature response (~6 K per 100 solar unit) appears at various altitudes at
315 55-65°S in July and August (Figure 4b).

316 Figure 4(c;d) shows the same as Figure 4(c;d) but with a Chebyshev type II high-pass filter having
317 a cutoff-period of 183-days applied to the temperature data. An apparent descent from 20-100 hPa in the
318 case of equatorial temperature and from the stratosphere to the troposphere in the case of high latitude
319 temperature can now be observed. Similarly, Figure 4(e;f) shows the same as Figure 4(c;d) but with a
320 Chebyshev type II band-pass filter having a bandwidth of 31 to 183 days applied to the temperature
321 data. Downward descent of the solar signals becomes clearer though only the high latitude signal
322 manages to cross the tropopause and move into the troposphere.

323 We found that the downward movement from the upper stratosphere to the lower stratosphere is
324 robust and becomes clearer when either a Chebyshev type I, or type II or Butterworth filter is applied to
325 the temperature data. Together, the signals suggest that during these seasons the high frequency
326 response in the stratosphere is characterized by warming in the tropics and cooling at high latitudes,
327 implying a slowing down of the BD-circulation. They also suggest that the effect moves gradually from
328 the upper stratosphere to the lower stratosphere. However, the downward movement of the signal into
329 the troposphere loses statistical significance when either a Chebyshev type I or Butterworth filter is
330 applied. When the cut-off period of the filter is increased beyond 6-months, the high latitude signals

331 become noticeably weaker (not shown). Thus, it remains to be verified whether or not the high latitude
332 temperature signal actually descends from the stratosphere into the troposphere in reality.

333 **[[Insert Figure 4 here]]**

334 To examine the variability of the solar signals in stratospheric temperature for HS and LS years
335 more closely, time series of the daily temperatures in the upper and lower stratosphere for each
336 individual year are shown in Figures 5 and 6, respectively. In Figure 5, daily mean temperature at 10
337 hPa averaged over the latitude ranges of 10-15°S (top row) and 55-65°S (bottom row) are compared for
338 HS (1st column) and LS (2nd column) conditions, where the averages are weighted by the cosines of the
339 latitudes.

340 **[[Insert Figure 5 here]]**

341 **[[Insert Figure 6 here]]**

342 Figure 5 shows that, in the upper stratosphere, considerable temperature variation exists and the
343 variance is larger for HS years than for LS years. The larger temperature variation under HS may be
344 partially due to the contaminating effects of the major SSW (year 2002, purple line) and the major
345 volcanic eruptions (years 1982, 1991 and 1992; blue lines). The 3rd- 4th columns of Figure 4, display the
346 mean daily temperatures under HS (red) and LS (grey) conditions for no filtering and 183-day
347 Chebyshev type II high-pass filter. The shaded regions represent 95% confidence intervals for the mean.
348 When the shaded regions do not overlap, it indicates that the average temperature differences between
349 the HS and LS groups are significant at the 95% confidence level. In order to focus on the 11-yr SC
350 effect, years affected by the SSW and major volcanic eruptions are excluded from the group mean in
351 HS. For equatorial temperature, statistically significant differences between HS and LS conditions are
352 evident for both the raw data and the high frequency component. For high latitude temperature, the
353 difference is only significant for the high frequency component. When the unfiltered data are used, it is
354 barely differentiable.

355 Figure 6 shows the corresponding temperature time series for the lower stratosphere at 50 hPa and
356 for the same latitude ranges as in Figure 5. It shows that higher temperatures existed for the volcanic
357 eruption affected years near the equator and subtropics, due to the warming effect of the volcanic
358 aerosols (Robock and Mao, 1992). In the 2002 winter, substantially lower temperatures are found at low
359 latitudes accompanied by higher temperatures at high latitudes. In the subtropics (top row), significant
360 positive temperature differences between HS and LS exist whether or not a filter is applied. The
361 response obtained by using raw unfiltered daily data is found from April to September while the high
362 frequency response occurs briefly only in August and September. The magnitude of the response is
363 larger in the unfiltered data than in the high frequency component. Conversely, the high latitude
364 temperature differences are only significant in the high frequency domain in July to early September.
365 The lack of significance in unfiltered high latitude temperature in the lower stratosphere is due to a
366 cancellation effect between high and low frequency components (not shown).

367 **3.2.2 Solar signals in zonal wind**

368 Figure 7 is similar to Figure 3 except that the temperature is replaced by the zonal-mean zonal
369 wind. The composite differences are the high frequency zonal-mean zonal wind between HS and LS
370 conditions (ΔU_{HS-LS}). The climatology of the wind field is characterized by a strengthening and
371 poleward movement of the stratospheric westerly jet from June to Mid-August and a gradual weakening
372 and downward movement of the jet thereafter. The high frequency ΔU_{HS-LS} signature is clearly marked
373 by a strengthening of the stratospheric jet as the significant westerly anomaly almost tracks the centre of
374 the jet. The signals originate in the subtropical upper stratosphere and lower mesosphere and then move
375 poleward and downward. There is a symmetric, but weaker, response in the NH subtropics (not shown),
376 which shows little poleward movement. As a whole, the overall structure of high frequency ΔU_{HS-LS} in
377 the stratosphere agrees exceedingly well with that proposed earlier by Kodera and Kuroda (2002) and is
378 consistent with the thermal wind balance in the presence of the anomalous latitudinal temperature
379 differences at 5-10 hPa shown in Figure 3.

380

[[Insert Figure 7 here]]

381 To examine the high frequency responses and variability of the wind in more detail, Figure 8 shows
382 the daily evolution of the zonal wind at 30-40°S, 5hPa (upper panels), and at 40-50°S, 50hPa (lower
383 panels) for HS (1st column) and LS (2nd column) conditions. Significant positive ΔU_{HS-LS} for the
384 unfiltered data exists only in Austral winter and only in the upper stratosphere winds. The difference is
385 noticeably enhanced both in the upper and lower stratosphere if a high-pass filter is applied. ΔU_{HS-LS}
386 becomes insignificant if data from 2002 are included.

387 **[[Insert Figure 8 here]]**

388 **3.3 Solar signal in the Sothern Annular Mode**

389 It is known that the changes in zonal-mean zonal wind in the tropospheric westerly jet during the
390 SH winter are affected by changes in wave forcing (Limpasuvan and Hartmann 2000; Lorenz and
391 Hartmann 2001) and the effects may be projected onto the large scale atmospheric mode, *i.e.* the
392 Southern Annular Mode (SAM) (Thompson *et al.* 2005). Figure 9 shows the running linear regression
393 (in SAM index per 100 solar unit) using raw daily SAM (a) and 183-day high-pass filtered SAM (b),
394 where the linear trend is removed and the data from 2002 and two years following the major volcanic
395 eruptions are excluded. An almost identical response pattern can be seen in (a) and (b), suggesting that
396 the SAM response to the 11-yr SC is dominated by the high frequency response. In the stratosphere, a
397 positive solar response originates at 1hPa and above in early July and descends towards the lower
398 stratosphere in July and August. A negative response is obtained from October near the stratopause.
399 Noisier but significant responses are also found in the troposphere. They are positive in June-July
400 preceding the stratospheric signal, negative during mid-winter, and positive again from October onward.
401 No consistent signals can be found in the low frequency domain (not shown).

402 **[[Insert Figure 9 here]]**

403 Figure 9 suggests that the 11-yr SC may project onto the tropospheric SAM in early winter or late
404 spring. To test whether there is any definite projection of the 11-yr SC on the SAM in the troposphere,
405 scatter plots of F_s versus the station-based monthly Marshall-SAM from 1957-2009 are shown in Figure
406 10. We found that, in both June and November, the correlations are not significantly separable from

407 zero either using the raw data, or in the high or low frequency domains. Similar results were obtained
408 for other months or seasonal averages. We also found that there is no significant difference in the
409 variance and the histogram of the SAM under HS and LS conditions in the SH winter and spring.

410 **[[Insert Figure 10 here]]**

411 **4. Discussion**

412 The most significant solar signature is the positive response of stratospheric temperature, consistent
413 with the theory that the interaction between solar UV and ozone photochemistry increases temperature
414 there (Haigh, 1994). However, the stratospheric signals of the 11-yr SC are sensitive to the
415 contamination of the 2002 SSW event and the major volcanic eruptions and zonal winds are more
416 sensitive than temperature. We have noted that the zonal wind response becomes noticeably clearer and
417 more significant by excluding the data from year 2002 or by separating the analysis into high and low
418 frequency components. The fact that the solar signal in zonal wind is more sensitive to sampling
419 methods than that in temperature implies that temperature is more directly affected by the variation of
420 solar output during the 11-yr SC. This is consistent with the known mechanism of solar UV-
421 stratospheric ozone interaction. In the troposphere, however, the solar signature in temperature is more
422 sensitive to the long-term trends than to the SSW or the major volcanic eruptions. Linearly removing the
423 trends enhances the signal in the troposphere and weakens the signals in the stratosphere. Without
424 removing a linear trend, up to 0.3°K of the temperature response in the low-latitude lower stratosphere
425 might be the result of aliasing of a long-term trend onto the solar signal and this is in good agreement
426 with Lu *et al.* (2007) and Frame and Gray (2010).

427 Here we have found that, during the SH winter, the 11-yr SC signals become stronger and
428 statistically more significant when the analysis is carried out at high and low frequencies than when the
429 raw data are used. The difference is more noticeable at high latitude as the high and low frequency
430 responses tend to cancel each other there. The cancelation partly explains why high latitude responses
431 are hard to detect statistically when raw data are used.

432 The difference in high and low frequency responses highlights new aspects of the underlying
433 physical processes. The static low frequency responses in the stratosphere may represent the slow
434 varying temperature and circulation change due to ozone transport induced by solar UV-stratospheric
435 ozone interaction and changes in BD-circulation (Kodera and Kuroda 2002; Gray *et al.* 2009; Gray *et al.*
436 2010). The non-static high frequency responses in temperature, zonal wind and the SAM to the 11-yr
437 SC and the fact that the signals are statistically significant only during SH winter point to a dynamic
438 effect of the 11-yr SC on the stratospheric circulation. These high frequency signals are generally
439 consistent with the dynamic response studied previous (Kodera and Kuroda 2002; Matthes *et al.* 2004;
440 Kuroda *et al.* 2007). It may be interpreted as a possible association between the 11-year solar cycle and
441 the temporal or seasonal persistence of the polar vortex and the BD-circulation. Apart from the known
442 mechanism of *in-situ* solar UV and ozone photochemistry interaction, other mechanisms may also be at
443 play to produce those stratospheric signals. For instance, the signature of the solar wind streaming out
444 from the Sun has also been found in various climate records (Lu *et al.* 2008b; Seppälä *et al.* 2009;
445 Lockwood *et al.*, 2010a,b; Woollings *et al.* 2010). Observational studies have shown that the solar wind
446 induced geomagnetic activity may alter stratospheric chemistry indirectly through energetic particle
447 precipitation (EPP) (Solomon *et al.* 1982; Randall *et al.*, 2005; 2007; Seppälä *et al.* 2007; Siskind *et al.*
448 2007). Chemical-dynamical coupled general circulation models (GCMs) have indicated that odd
449 nitrogen (NO_x) induced by energetic charged particle precipitation during geomagnetic storms may
450 cause temperature changes in both the polar and equatorial regions and in the stratosphere and the
451 troposphere (Langematz *et al.* 2005; Rozanov *et al.* 2005). Lu *et al.* (2007) found that the magnitude of
452 temperature response in the low latitude lower stratosphere to geomagnetic activity was slightly larger
453 than that associated with the 11-yr SC and that the temperature response to the 11-yr SC and
454 geomagnetic Ap index tend to enhance each other. Lu *et al.* (2008b) have shown that there is a robust
455 relationship between solar wind dynamic pressure and the zonal wind and temperature in the northern
456 polar winter. Stratospheric wind and temperature variations are positively projected onto the Northern
457 Annular Mode (NAM) when the 11-yr SC is at its maximum phase, and negatively projected onto the
458 NAM during the 11-yr SC minimum phase. A weakening of the BD-circulation with reduced upwelling

459 into the lower stratosphere at low-latitude under high solar wind forcing is consistent with the behavior
460 of the high frequency response shown here. Our rationale is that, at solar maximum, a warming effect in
461 the low latitude stratosphere due to solar UV-stratospheric ozone interaction together with a cooling
462 effect in the high latitude stratosphere due to solar wind driven geomagnetic activity would enhance the
463 equator to pole temperature gradient. When both mechanisms work together, it would result in a
464 stronger dynamic effect on the stratospheric circulation than that resulting from just one of these two
465 mechanisms. Given that the 11-yr SC signals are found to be opposite at high latitudes, it may therefore
466 be speculated that the high frequency responses represent a combined effect of enhanced solar UV,
467 which causes warming near the equatorial stratosphere, and solar wind driven processes, which cause
468 cooling at high latitude stratosphere. This may also explain the static high frequency temperature
469 response in the lower stratosphere (~70 hPa) which seems to be independent of those originated in the
470 upper stratosphere (see Figures 3 and 4). Nevertheless, it remains to be understood what mechanism has
471 caused the cooling effect in the high latitude stratosphere in relation to solar wind activity. Recent
472 studies have suggested that the EPP-NO_x and its downward decent during winter and spring play an
473 insignificant role on stratospheric ozone and circulation (Lu *et al.* 2008a; Salmi *et al.* 2011). Lu *et al.*
474 (2008a) suggested that changes observed in stratospheric winds and temperatures were unlikely caused
475 by photochemistry associated with EPP-NO_x and stratospheric ozone but were more likely due to an
476 indirect dynamical link, *e.g.* changes in wave activity, as they found that the spring temperature and
477 wind variations in relation to changes of geomagnetic Ap index have a sign that is opposite to that
478 expected from the NO_x-ozone photochemistry mechanism.

479 The modulating effect of the QBO has not been explicitly studied here due to the limited data
480 records. Nevertheless, our analysis indicates that the QBO may add noticeable contamination to the
481 signals in the temperature near the equatorial stratosphere at 20-30 hPa if no high and low frequency
482 separation is made for the solar signature. This agrees well with the findings of Smith and Matthes
483 (2008). Here, we also found that separating the response into high and low frequency components not
484 only allows isolation of the fast and slow responses but also partially eliminates the QBO contamination
485 at those pressure levels. However, unlike the Northern Hemisphere where a significant solar signature

486 can only be detected when the data are subgrouped according to the QBO phases (*e.g.* Labitzke and van
487 Loon 1988; Lu *et al.* 2009), it is not essential to separate the data according to the QBO phases in order
488 to obtain significant 11-yr SC signal in the Southern Hemisphere.

489 The low frequency responses (> 36 months) are found in the lower stratosphere temperature
490 extending from the North Pole to the South Pole with the signal becoming weaker at mid-latitudes.
491 These low frequency responses could be related to slowly-varying transported ozone anomalies as
492 suggested by Austin *et al.* (2008) and Gray *et al.* (2009). They may also be partially associated with a
493 downward movement of ozone-UV interaction in the upper to middle stratosphere due to a change in the
494 BD-circulation and such a process could account for up to 1 K per solar unit in the observed increase in
495 temperature near the equatorial lower stratosphere (see Figure 4(a;c;e)). Other slow processes such as
496 thermal inertia of the oceans may also play a role (Austin *et al.* 2008; White *et al.* 2003; White and Liu
497 2008).

498 In the troposphere, we found the zonally averaged solar signals are generally more fragmented than
499 those in the stratosphere. At high frequency, there are some indications of downward propagation of
500 solar signals from the stratosphere into the troposphere at high latitudes (see Figure 4 and 7). However,
501 the most significant signal in temperature is a positive response at 30-50° and this can only be obtained
502 when the long-term trend is removed (see figure 2) and is consistent with previous studies (van Loon
503 and Labitzke 1998; Haigh *et al.* 2005; Gleisner and Thejll 2003; Crooks and Gray 2005; Lu *et al.* 2007;
504 Frame and Gray 2010). A significant signal in tropospheric zonal winds was found only in the low
505 frequency domain. The signal is characterized by a weakening of the sub-tropical jet and the effect is
506 symmetric about the equator, consistent with Haigh *et al.* (2005). The magnitude and spatial structure of
507 the signal in tropospheric zonal wind ($\sim 1-2$ m/s) is in general agreement with the model simulations of
508 Haigh *et al.* (2005; 2006) and Simpson *et al.* (2009), where a positive equator-to-pole temperature
509 gradient was applied in the lower stratosphere. Nevertheless, we have noted that the positive signal in
510 the tropical lower stratosphere / troposphere is much weaker in ECMWF data than those imposed in the
511 model simulations.

512 It has also been suggested that higher solar forcing may cause stronger upward motion in the winter
513 hemisphere subtropics and enhanced downward motion in the summer hemisphere subtropics (van Loon
514 *et al.* 2004; Meehl *et al.* 2008). This response is associated with the “bottom-up” mechanism that is not
515 symmetric about the equator and is longitudinally varying and confined mostly to the Pacific Ocean
516 (Meehl *et al.* 2003; van Loon *et al.* 2007). As our analysis here has mainly focused on the zonal pattern
517 of the signals, our results cannot be directly compared to those reported by Meehl *et al.* (2003; 2008).
518 Using a stratosphere-troposphere coupled GCM, Meehl *et al.* (2009) show that both “top-down” and
519 “bottom-up” mechanisms may work together to induce positive feedbacks in the ocean-atmosphere
520 system that may amplify the response to solar irradiance variations. Further studies are needed to
521 understand how the stratospherically originating changes may amplify the longitudinal variations
522 associated with air-sea interaction in the tropical troposphere.

523 Linear regression between the 11-yr SC and the SAM shows that the solar signal is marked by a
524 strengthening of the stratospheric SAM during winter and a weakening of the SAM in the uppermost
525 stratosphere during spring. However, an 11-yr solar cycle influence in the stratosphere as a cause of
526 change in the tropospheric SAM cannot be established directly or linearly for the extended period of
527 1957-2009; other modulating factors, *e.g.* the QBO, must be taken into account to reveal any significant
528 solar effect on the tropospheric SAM. This is consistent with the results of Roscoe and Haigh (2007)
529 based upon multi-regression analysis where they also used station based Marshall SAM and found that
530 the 11-yr SC signal is not significant. However, a QBO modulation of the polar vortex may itself be
531 modified by the 11-year cycle of solar activity (Labitzke 2003; Salby and Callaghan 2006) and this
532 combined solar-QBO effect has been detected in the SAM by using a composite solar-QBO (SQBO)
533 index for the period of 1958-2006 (Roscoe and Haigh 2007). They showed that SQBO was able to
534 capture more variance in the SAM than the QBO and the 11-yr SC alone and suggested that the effect of
535 the 11-yr SC on the tropospheric SAM is non-linear and is modulated by the QBO. Indeed, the
536 modulation effects of the QBO and the 11-yr SC on the SAM have been studied by Kuroda and Kodera
537 (2005), Kuroda and Shibata (2006) and Kuroda and Yamazaki (2010). As our primary goal here is to
538 study whether or not there is a direct projection of the 11-yr SC on the SAM and also as we are limited

539 by the amount of data available, we have not studied the *modulation* effects either by the 11-yr SC or by
540 the QBO on the SAM. Therefore, our results are not directly comparable to either the signal of SQBO
541 shown by Roscoe and Haigh (2007) or the QBO or solar modulated SAM patterns studied by Kuroda
542 and co-authors. In addition to aliasing effects of the QBO, long-term trend, volcanoes and the 2002-
543 SSW, the signals could also be affected by ENSO, which may be also related to non-linear effects (*e.g.*
544 Marsh and Garcia, 2007; Calvo *et al.* 2009). Again, due to the limited data available, those effects were
545 not studied here.

546 To check whether or not the signals presented here may have been affected by merging two
547 different data sets together, we have also performed the same analysis by excluding the ECMWF
548 Operational data from our analysis and have found that the results remain qualitatively similar. For the
549 high frequency response, both temperature and zonal wind responses in fact become larger in magnitude
550 though the significant regions remain similar due to a smaller sample size. For the low frequency
551 response, the spatial pattern of the response remains similar but the regions covered by the 95%
552 confidence levels reduce. We also performed the same analysis by including data back to 1968 as
553 Kuroda and Yamazaki (2010) had done. Again the spatial patterns of the solar signals are generally
554 similar though the magnitude of the high frequency response reduces significantly. Thus, the results
555 presented here should be verified in the future, when longer data sets become available. This applies in
556 particular to the upper stratosphere where the impacts of discontinuities are more marked and in the
557 troposphere where the magnitude of the response is small and comparable to the uncertainty range
558 associated with the ECWMF reanalysis data (Uppala *et al.* 2005).

559 **5. Conclusions**

560 We have studied the characterization of 11-yr SC signals in the SH atmosphere during the winter and
561 spring using ECMWF daily and monthly data from 1979 to 2009. By separating the response into high
562 (< 6 months) and low (>36 months) frequency domains, we have found:

563 1) The 11-yr SC signal is generally more robust in temperature than in zonal wind.

- 564 2) Spatially different 11-yr SC signals exist at high (< 6 months) and low (> 36 months) frequency
565 domains. In the stratosphere, the high and low frequency responses tend to enhance each other
566 near the equator and subtropics, while they oppose one another at high latitudes.
- 567 3) The high frequency response in the stratosphere is marked by an enhanced latitudinal
568 temperature gradient in HS years from the equator to pole and a strengthened stratospheric jet
569 during winter. The response moves poleward and downward from the upper stratosphere to the
570 lower stratosphere by tracking the movement of the stratospheric jet, as noted by Kodera and
571 Kuroda (2002).
- 572 4) In the lower stratosphere, the positive response of temperature to the 11-yr SC is dominated by
573 its low frequency component.
- 574 5) In the stratosphere, the magnitude and the statistical significance of temperature and zonal wind
575 responses to the 11-yr SC are sensitive to the contamination of the 2002 SSW event and major
576 volcanic eruptions but the general spatial pattern of the responses remains similar with or
577 without these data.
- 578 6) In the troposphere, the responses in the high and low frequency domains are of opposite signs
579 but only the low frequency response with warmer temperatures in HS years is significant
580 (figure 2). The low frequency latitudinal temperature gradients and the resulting zonal wind
581 anomalies are consistent with the results of Haigh et al (2005).
- 582 7) In the troposphere, the solar signature in temperature is more sensitive to the long-term trend
583 than to the SSW or the major volcanic eruptions. Linearly removing the trend enhances the
584 signal in the troposphere and weakens the signature in the stratosphere.
- 585 8) A significant projection of the 11-yr SC onto the SAM can only be detected in the stratosphere
586 and in the high frequency component. The signal is marked by a strengthening of the
587 stratospheric SAM during winter and a weakening of the SAM in the uppermost stratosphere
588 during spring.

589

590 **Acknowledgements**

591 **Acknowledgements:** HL and MJJ were supported by the UK Natural Environment Research Council
592 (NERC). LJG was supported by the UK NERC National Centre for Atmospheric Science (NCAS).
593 MPB was funded by NSF under the US CLIVAR program and the Office of Polar Programs. Finally,
594 we thank two anonymous reviewers for their detailed and constructive comments on the original version
595 of the manuscript.

596

597 **References**

- 598 Austin J. et al. 2008. Coupled chemistry climate model simulations of the solar cycle in ozone and temperature. *J.*
599 *Geophys. Res.* **113**: D11306, doi:10.1029/2007JD009391.
- 600 Baldwin MP, Thompson DWJ. 2009. A critical comparison of stratosphere-troposphere coupling indices, *Q. J. R.*
601 *Meteorol. Soc.* **135**: 1661-1672.
- 602 Calvo N, Giorgetta MA, Garcia-Herrera R, Manzini E. 2009. Nonlinearity of the combined warm ENSO and QBO
603 effects on the northern hemisphere polar vortex in MAECHAM5 simulations. *J. Geophys. Res.*, **114**:
604 doi:10.1029/2008JD011,445.
- 605 Charlton AJ, O'Neill A, Lahoz WA, Berrisford P. 2005. The splitting of the stratospheric polar vortex in the
606 southern hemisphere, September 2002: Dynamical evolution. *J. Atmos. Sci.* **62**: 590– 602.
- 607 Claud C, Cagnazzo C, Keckhut P. 2008. The effect of the 11-year solar cycle on the temperature in the lower
608 stratosphere. *J. Atmos. Sol.-Terr. Phys.* **70**: 2031–2040.
- 609 Cnossen I, Lu H, Bell CJ, Gray LJ, Joshi MM. 2010. Solar signal propagation: the role of gravity waves and
610 stratospheric sudden warmings. *J. Geophys. Res.* **116**: D02118, doi:10.1029/2010JD014535.
- 611 Coughlin KT, Tung KK. 2004. 11-year solar cycle in the stratosphere extracted by the empirical mode
612 decomposition method, in *Solar Variability and Climate Change*, edited, pp. 323-329, PERGAMON-ELSEVIER
613 SCIENCE LTD, Killington.
- 614 Crooks SA, Gray LJ. 2005. Characterization of the 11-year solar signal using a multiple regression analysis of the
615 ERA-40 dataset. *J. Clim.* **18**: 996-1015.
- 616 Gleisner H, Thejll P. 2003. Patterns of tropospheric response to solar variability. *Geophys. Res. Lett.* **30**: L1711,
617 doi:10.1029/2003GL017129.
- 618 Frame THA, Gray LJ. 2010. The 11-year solar cycle in ERA-40 data: an update to 2008. *J. Clim.* **23**, 2213-2222.
- 619 Gray LJ, Crooks SA, Pascoe CA, Sparrow S, Palmer M. 2004. Solar and QBO influences on the timing of
620 stratospheric sudden warmings. *J. Atmos. Sci.* **61**: 2777-2796.
- 621 Gray LJ, Rumbold ST, Shine KP. 2009. Stratospheric temperature and radiative forcing response to the 11-year
622 solar cycle changes in irradiance and ozone. *J. Atmos. Sci.* (in press).
- 623 Gray LJ, Beer J, Geller M, Haigh JD, Lockwood M, Matthes K, Cubasch U, Fleitmann D, Harrison G, Hood L,
624 Luterbacher J, Meehl GA, Shindell D, van Geel B, White W. 2010. Solar influence on climate. *Rev. Geophys.*
625 doi:10.1029/2009RG000282.
- 626 Haigh JD. 1994. The role of stratospheric ozone in modulating the solar radiative forcing of climate. *Nature*,
627 **370**:544-546.
- 628 Haigh JD. 2003. The effects of solar variability on the Earth's climate. *Philos. Trans. R. Soc. Lond. Ser. A-Math.*
629 *Phys. Eng. Sci.* **361**: 95-111.
- 630 Haigh JD, Blackburn M, Day R. 2005. The response of tropospheric circulation to perturbations in lower
631 stratospheric temperature. *J. Clim.* **18**: 3672–3691.

632 Haigh JD, Blackburn M. 2006. Solar influences on dynamical coupling between the stratosphere and troposphere.
633 *Space Sci. Rev.* **125**: 331–344.

634 Hameed S, Lee JN. 2005. A mechanism for sun-climate connection. *Geophys. Res. Lett.* **32**: L23817,
635 doi:10.1029/2005GL024393.

636 Hood LL, Soukharev BE. 2006. Solar induced variations of odd nitrogen: Multiple regression analysis of UARS
637 HALOE data, *Geophys. Res. Lett.* **33**: L22805, doi:10.1029/2006GL028122.

638 Keckhut P, Cagnazzo C, Chanin ML, Claud C, Hauchecorne A. 2005. The 11-year solar-cycle effects on
639 temperature in the upper stratosphere and mesosphere Part I: Assessment of observations. *J. Atmos. Sol.-*
640 *Terr. Phys.* **67**: 940–947.

641 Kodera K, Kuroda Y. 2002. Dynamical response to the solar cycle. *J. Geophys. Res.* **107**: D4749,
642 doi:4710.1029/2002JD002224.

643 Kodera K, Matthes K, Shibata K, Langematz U, Kuroda Y. 2003. Solar impact on the lower mesospheric subtropical
644 jet: A comparative study with general circulation model simulations. *Geophys. Res. Lett.* **30**: L1315,
645 doi:10.1029/2002GL016124.

646 Kodera K. 2004. Solar influence on the Indian Ocean Monsoon through dynamical processes. *Geophys. Res. Lett.*
647 **31**: L24209, doi:10.1029/2004GL020928.

648 Kodera K, Shibata K. 2006. Solar influence on the tropical stratosphere and troposphere in the northern summer,
649 *Geophys. Res. Lett.* **33**: L19704, doi:10.1029/2006GL026659.

650 Kodera K, Hori ME, Yukimoto S, Sigmond M. 2008. Solar modulation of the Northern Hemisphere winter trends
651 and its implications with increasing CO₂. *Geophys. Res. Lett.*, **35**: L03704, doi:10.1029/2007GL031958.

652 Kuroda Y, Deushi M, Shibata K. 2007. Role of solar activity in the troposphere-stratosphere coupling in the
653 Southern Hemisphere winter. *Geophys. Res. Lett.* **34**: L21704, doi:10.1029/2007GL030983.

654 Kuroda Y, Kodera K. 2002. Effect of solar activity on the Polar-night jet oscillation in the northern and southern
655 hemisphere winter. *J. Meteorol. Soc. Jpn.* **80**: 973-984.

656 Kuroda Y, Kodera K. 2005. Solar cycle modulation of the Southern Annular Mode. *Geophys. Res. Lett.* **32**: L13802,
657 doi:10.1029/2005GL022516.

658 Kuroda Y, Shibata K. 2006. Simulation of solar-cycle modulation of the Southern Annular Mode using a chemistry-
659 climate model, *Geophys. Res. Lett.*, **33**: L05703, doi:10.1029/2005GL025095.

660 Kuroda Y, Yamazaki K. 2010. Influence of the solar cycle and QBO modulation on the Southern Annular Mode,
661 *Geophys. Res. Lett.* **32**: L12703, doi:10.1029/2010GL043252.

662 Langematz U, Grenfell JL, Matthes K, Mieth P, Kunze M, Steil B, Brühl C. 2005. Chemical effects in 11-year solar
663 cycle simulations with the Freie Universität Berlin Climate Middle Atmosphere Model with online chemistry
664 (FUB-CMAM-CHEM). *Geophys. Res. Lett.* **32**: L13803, doi:13810.11029/12005GL022686.

665 Labitzke K. 2002. The solar signal of the 11-year sunspot cycle in the stratosphere: Differences between the
666 Northern and Southern summers. *J. Meteorol. Soc. Jpn.* **80**: 963-971.

667 Labitzke K. 2003. The global signal of the 11-year sunspot cycle in the atmosphere: When do we need the QBO?
668 *Meteorol. Zeitschrift* **12**: 209-216.

669 Labitzke K, van Loon H. (1988), Associations between the 11-year solar cycle, the QBO and the atmosphere, Part
670 I: The troposphere and stratosphere in the northern hemisphere in winter. *J. Atmos. Terr. Phys.* **50**: 197-206.

671 Limpasuvan V, Hartmann DL. 2000. Wave-maintained annular modes of climate variability. *J. Clim.* **13**: 14414-
672 4429.

673 Lockwood M, Bell C. Woollings T, Harrison RG, Gray LJ, Haigh JD. 2010a. Top-down solar modulation of climate:
674 Evidence for centennial-scale change. *Environ. Res. Lett.* **5**: 034008, doi:034010.031088/031748-
675 039326/034005/034003/034008.

676 Lockwood M, Harrison RG, Woollings T, Solanki SK. 2010b. Are cold winters in Europe associated with low solar
677 activity? *Environ. Res. Lett.* **5**: 024001.

678 Lorenz, D. J., D. L. Hartmann 2001. Eddy-zonal flow feedback in the Southern Hemisphere. *J. Atmos. Sci.* **58**: 3312-
679 3327.

680 Lu H, Jarvis MJ, Graf H-F, Young PC, Horne RB. 2007. Atmospheric temperature response to solar irradiance and
681 geomagnetic activity. *J. Geophys. Res.* **112**: D11109. DOI: 11110.11029/12006JD007864.

682 Lu H, Clilverd M, Seppälä A, Hood L. 2008. Geomagnetic perturbations on stratospheric circulation in late winter
683 and spring, *J. Geophys. Res.* **113**: D16106, doi:10.1029/2007JD008915.

684 Lu H, Jarvis MJ, Hibbins RE 2008. Possible solar wind effect on the Northern Annular Mode and northern
685 hemispheric circulation during winter and spring, *J. Geophys. Res.*, **113**: D23104,
686 doi:23110.21029/12008JD010848.

687 Lu H, Gray LJ, Baldwin MP, Jarvis MJ. 2009. Life cycle of the QBO-modulated 11-year solar cycle signals in the
688 Northern Hemispheric winter. *Q. J. R. Meteorol. Soc.*, **135**: 1030-1043.

689 Marsh DR, Garcia RR. 2007. Attribution of decadal variability in lower stratospheric tropical ozone, *Geophys. Res.*
690 *Let.*, **34**: L21807, doi:10.1029/2007GL030935.

691 Matthes K, Langematz U, Gray LJ, Kodera K, Labitzke K. 2004. Improved 11-year solar signal in the Freie
692 Universität Berlin Climate Middle Atmosphere Model (FUB-CMAM). *J. Geophys. Res.* **109**: D06101,
693 doi:06110.01029/02003JD004012.

694 Matthes K, Kuroda Y, Kodera K, Langematz U. 2006. Transfer of the solar signal from the stratosphere to the
695 troposphere: Northern winter. *J. Geophys. Res.* **111**: D06108, doi:06110.01029/02005JD006283.

696 Meehl GA, Washington WM, Wigley TML, Arblaster JM, Dai A. 2003. Solar and greenhouse gas forcing and
697 climate response in the twentieth century. *J. Clim.* **16**: 426-444.

698 Meehl GA, Arblaster JM, Branstator G, van Loon H. 2008. A coupled air-sea response mechanism to solar forcing
699 in the pacific region. *J. Clim.* **21**: 2883-2897.

700 Meehl GA, Arblaster JM, Matthes K, Sassi F, van Loon H. 2009. Amplifying the pacific climate system response to
701 a small 11-year solar cycle forcing, *Science*, **325**: 1114, DOI: 10.1126/science.1172872.

702 Robock A., Mao J. 1992. Winter warming from large volcanic eruptions, *Geophys. Res. Lett.* **19**(24): 2405-2408.

703 Roscoe HK, Haigh JD. 2007. Influences of ozone depletion, the solar cycle and the QBO on the Southern Annular
704 Mode, *Q. J. R. Meteorol. Soc.* **133**:1855-1864.

705 Rozanov E, Callis L, Schlesinger M, Yang F, Andronova N, Zubov V. 2005. Atmospheric response to NO_y source due
706 to energetic electron precipitation. *Geophys. Res. Lett.* **32**(14): L14811, doi:10.1029/2005GL023041.

707 Salmi SM, Verronen PT, L. Thölix L, Kyrölä E, Backman L, Karpechko, AY, Seppälä A. 2011. Mesosphere-to-
708 stratosphere descent of odd nitrogen in February–March 2009 after sudden stratospheric warming. *Atmos.*
709 *Chem. Phys. Discuss.* **11**: 1429–1455.

710 Seppälä A, Randall CE, Clilverd MA, Rozanov E, Rodger CJ. 2009. Geomagnetic activity and polar surface air
711 temperature variability. *J. Geophys. Res.* **114**: A10312, doi:10.1029/2008JA014029.

712 Seppälä A, Verronen PT, Clilverd MA, Randall CE, Tamminen J, Sofieva V, Backman L, Kyrölä E. 2007. Arctic and
713 Antarctic polar winter NO_x and energetic particle precipitation in 2002-2006. *Geophys. Res. Lett.* **34**: L12810,
714 doi:10.1029/2007GL029733.

715 Siskind DE, Eckermann SD, Coy L, McCormack JP, Randall CE. 2007. On recent interannual variability of the Arctic
716 winter mesosphere: Implications for tracer descent. *Geophys. Res. Lett.* **34**: L09806,
717 doi:10.1029/2007GL029293.

718 Solomon S, Crutzen PJ, Roble RG. 1982. Photochemical coupling between the thermosphere and the lower
719 atmosphere: 1. Odd nitrogen from 50 to 120 km. *J. Geophys. Res.* **87**: 7206-7220.

720 Salby ML, Callaghan PF. 2006. Relationship of the quasi-biennial oscillation to the stratospheric signature of the
721 solar cycle. *J. Geophys. Res.* **111**: D06110, doi:10.1029/2005JD006012.

722 Scaife AA, Jackson DR, Swinbank R, Butchart N, Thornton HE, Keil M, Henderson L. 2005. Stratospheric
723 vacillations and the major warming over Antarctica in 2002. *J. Atmos. Sci.* **62**: 629-639.

724 Simpson IR, Blackburn M, Haigh JD. 2009. The role of eddies in driving the tropospheric response to stratospheric
725 heating perturbations. *J. Atmos. Sci.* **66**, 1347-1365.

726 Smith AK, Matthes K. 2008. Decadal-scale periodicities in the stratosphere associated with the solar cycle and the
727 QBO. *J. Geophys. Res.* **113**: D05311, doi:10.1029/2007JD009051.

728 Smith, SW.1997. The scientist and engineer's guide to digital signal processing, California Technical Publishing,
729 San Diego, pp625.

730 SPARC CCMVal Report on the Evaluation of Chemistry-Climate Models, 2010. V. Eyring, T. G. Shepherd, D. W.
731 Waugh (Eds.), SPARC Report No. 5, WCRP-X, WMO/TD-No. X,
732 <http://www.atmosp.physics.utoronto.ca/SPARC>.

733 Thompson DWJ, Baldwin MP, Solomon S. 2005. Stratosphere-troposphere coupling in the Southern Hemisphere.
734 *J. Atmos. Sci.* **62**: 708-715.

735 Uppala SM *et al.* 2005. The ERA-40 reanalysis. *Q. J. R. Meteorol. Soc.* **131**: 2961-3012.

736 van Loon H, Labitzke K. 1994. The 10–12 year atmospheric oscillation, *Meteorol. Z.* **3**: 259-266.

737 van Loon H, Labitzke K. 1998. The global range of the stratospheric decadal wave. Part I: Its association with the
738 sunspot cycle in summer and in the annual mean, and with the troposphere. *J. Clim.* **11**: 1529-1537.

739 van Loon H, Meehl GA, Arblaster JM. 2004. A decadal solar effect in the tropics in July-August. *J. Atmos. Sol.-Terr.*
740 *Phys.* **66**: 1767-1778.

741 van Loon H, Meehl GA, Shea DJ. 2007. Coupled air-sea response to solar forcing in the Pacific region during
742 northern winter. *J. Geophys. Res.* **112**: D02108, doi:02110.01029/02006JD007378.

743 van Loon H, Meehl GA. 2008. The response in the Pacific to the sun's decadal peaks and contrasts to cold events
744 in the Southern Oscillation. *J. Atmos. Sol.-Terr. Phys.* **70**: 1046-1055.

745 White WB, Dettinger MD, Cayan DR. 2003. Sources of global warming in the upper-ocean on decadal period
746 scales. *J. Geophys. Res.* **108(C8)**: 3248, doi:10.1029/2002JC001396.

747 White WB, Liu Z. 2008. Resonant response of the quasi-decadal oscillation to the 11-yr period signal in the Sun's
748 irradiance. *J. Geophys. Res.* **113**: C01002, doi:10.1029/2006JC004057.

749 Woollings T, Lockwood M, Masato G, Bell C, Gray L. 2010. Enhanced signature of solar variability in Eurasian
750 winter climate. *Geophys. Res. Lett.* **37**: L20805, doi:20810.21029/22010GL044601.

751

752 **Figure captions**

753 **Figure 1.** Composite differences (high solar –low solar (HS-LS)) of zonal-mean temperature (a;b;c;d)
754 and zonal wind (e;f;g;h) for June-August averages. In cases (a;e), all data from 1979-2009 are included.
755 In cases (b;f), data from year 2002 are excluded. In cases (c;g), years affected by the major volcanic
756 eruptions (*i.e.* 1982, 1983, 1992, and 1993) are excluded. In cases (d;h), data from 2002 and years
757 affected by the major volcanic eruptions are excluded. Statistical confidence levels above 95% are
758 shown as dashed grey contours.

759 **Figure 2.** Composite differences (high solar –low solar (HS-LS)) of zonal-mean temperature (a;b;c) and
760 zonal wind (d;e;f) for June-August averages. In cases (a;d), a Chebyshev type II high-pass filter with a
761 cutoff-period of 6-month is applied. In cases (b;e), a Chebyshev type I low-pass filter with a 36-month
762 cutoff period is used. In cases (c;f), temperature and zonal wind are linearly detrended first and then a
763 Chebyshev type I low pass filter with 36-month cutoff period is applied. Statistical confidence levels
764 above 95% are shown as dashed grey contours.

765 **Figure 3.** Left: monthly climatology zonal-mean zonal temperature (in units of K) for June to October
766 (top to bottom), displayed as lined contour plots in meridional-height cross section from 30°N to 90°N
767 and from 1000 hPa to 1 hPa. Right: same as the left panels but displayed as coloured contour plots for
768 the composite differences of the temperature between high solar and low solar conditions (HS-LS). The
769 areas enclosed within the grey lines indicate that the differences are statistically significant from zero
770 with a confidence level of 95% or above, calculated using a Monte-Carlo trial based non-parametric
771 test. Data which might be affected by the major volcanic eruptions and 2002 stratospheric major
772 warming are excluded.

773 **Figure 4.** Time vs pressure level plot of linear running regression (in K per 100 F10.7-cm solar flux
774 unit) between F_s and equatorial temperature averaged over 5°N to 5°S (a;c;e, where the contour interval
775 is ± 0.5 K) and temperature averaged over 55–65°S (b;d;f, where the contour interval is ± 2 K). In (a;b),
776 raw daily temperature is used. In (c;d), a high-pass filter with a cutoff-period of 183-days is applied to
777 the daily temperature. In (e;f), a bandpass filter with a bandwidth of 31 to 183 days is applied to the

778 daily temperature. An order 6 Chebyshev type II with passband ripple of 2 decibels is used for (c;d;e;f).
779 For all cases, the temperatures are linearly detrended first and the data from 2002, 1982, 1983, 1991 and
780 1992 are excluded from the regression. Statistical confidence levels above 90% and 95% are shown as
781 light and dark shadings.

782 **Figure 5.** Daily averaged zonal-mean temperatures (K) at 10 hPa, averaged over 0-5°S (1st row) and
783 over 55-65°S (2nd row), for HS (1st column), LS (2nd column) together with daily mean values for HS
784 (the line with red shading) and LS (the line with grey shading) conditions (3rd column). The daily mean
785 values for HS and LS at high frequency (< 183-days) estimated using a Chebyshev type II filter (4th
786 column) are also shown. The shaded regions represent the 95% confidence intervals of the mean. In the
787 HS group, the years in which data might be affected by the major volcanic eruptions are shown as blue
788 lines and the 2002 data are shown as the purple line. The daily mean values are calculated by excluding
789 major volcanic eruptions affected year and 2002 data.

790 **Figure 6.** As in Figure 5 but for temperatures at 50 hPa, averaged over latitude ranges of 10-15°S (1st
791 row) and 55-65°S (2nd row).

792 **Figure 7.** As in Figure 3 but the zonal-mean temperature is replaced by the zonal-mean zonal wind in
793 units of m s^{-1} .

794 **Figure 8.** As in Figure 5 but for zonal-mean zonal wind (m s^{-1}) at 30-40°S, 5hPa (1st row), and at 40-
795 50°S, 50hPa (2nd row).

796 **Figure 9.** As in Figure 4 but for the SAM derived from ECMWF daily data. (a) uses the raw daily
797 SAM; (b) a 183-day high-pass filter is applied to the SAM. The treatment of data and use of filter, lines
798 and shadings are the same as for Figure 4 and the contour interval is 0.25 SAM index per 100 solar unit.

799 **Figure 10.** (a;b) Scatter plot of F_s and July Marshall-SAM index. (c;d) Scatter plot of F_s and November
800 Marshall-SAM index. For (a;c) no filtering is applied to the data; for (b;d) a high-pass filter of 6-month
801 is applied to the data.

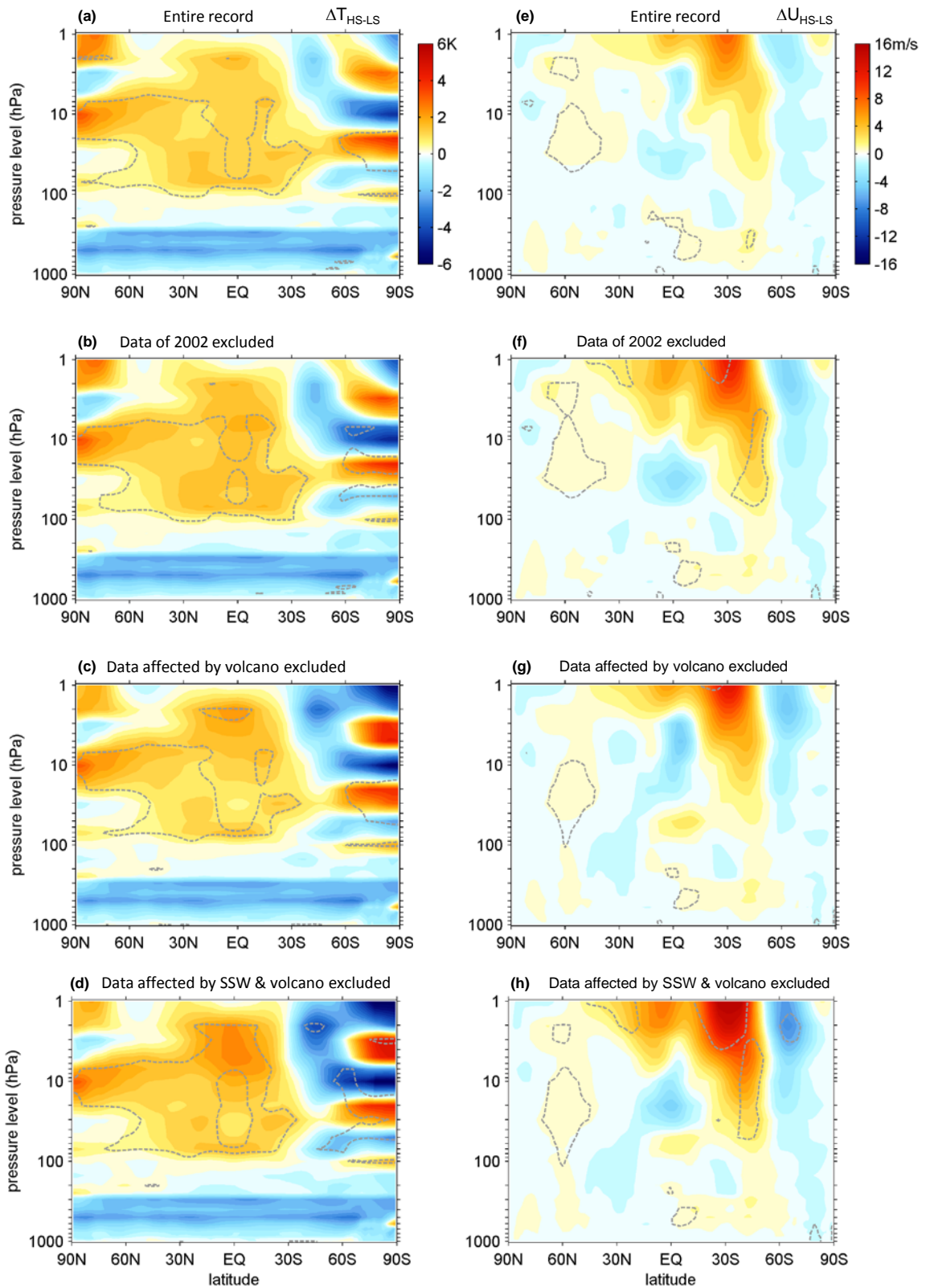


Figure 1

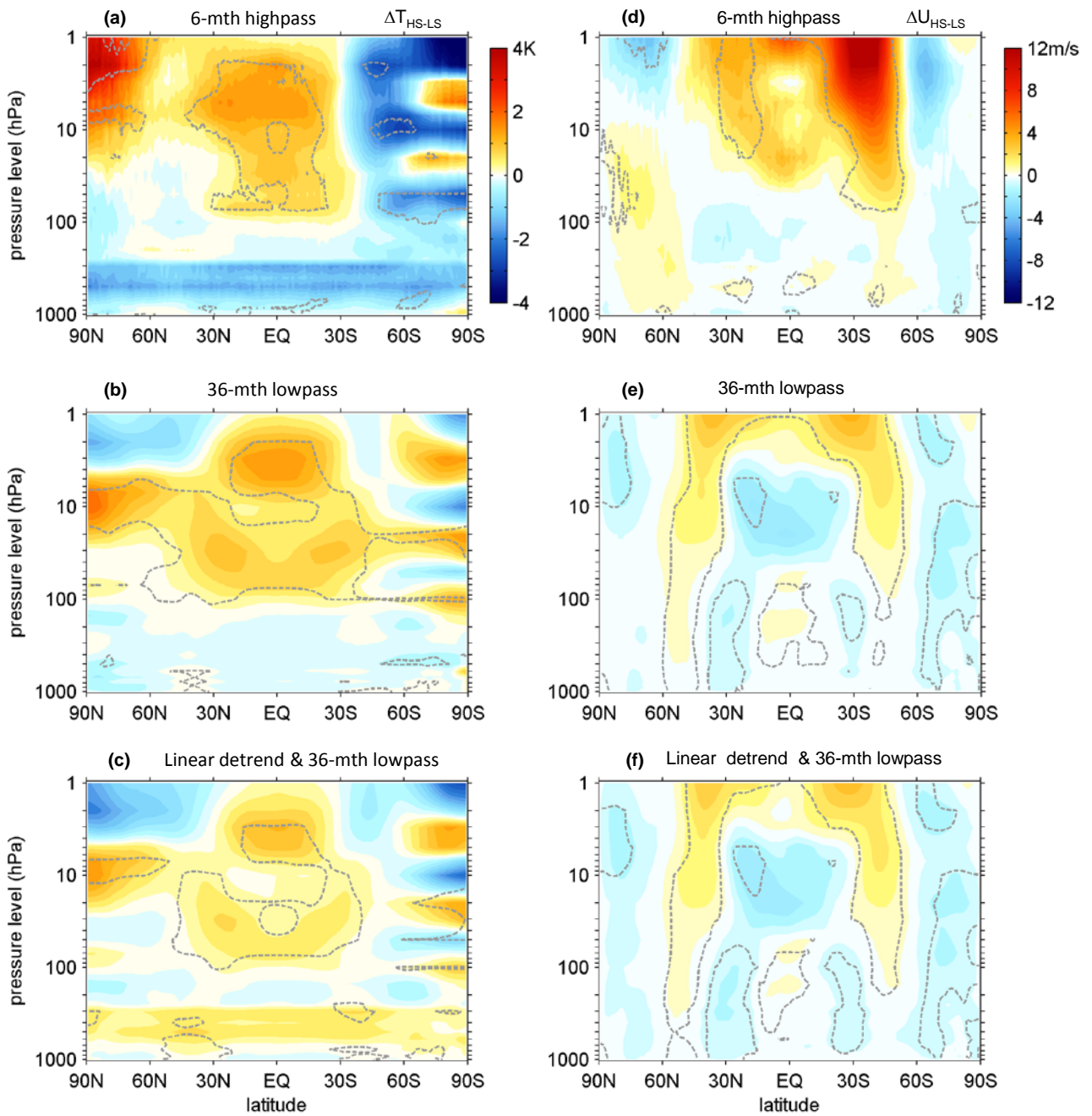


Figure 2

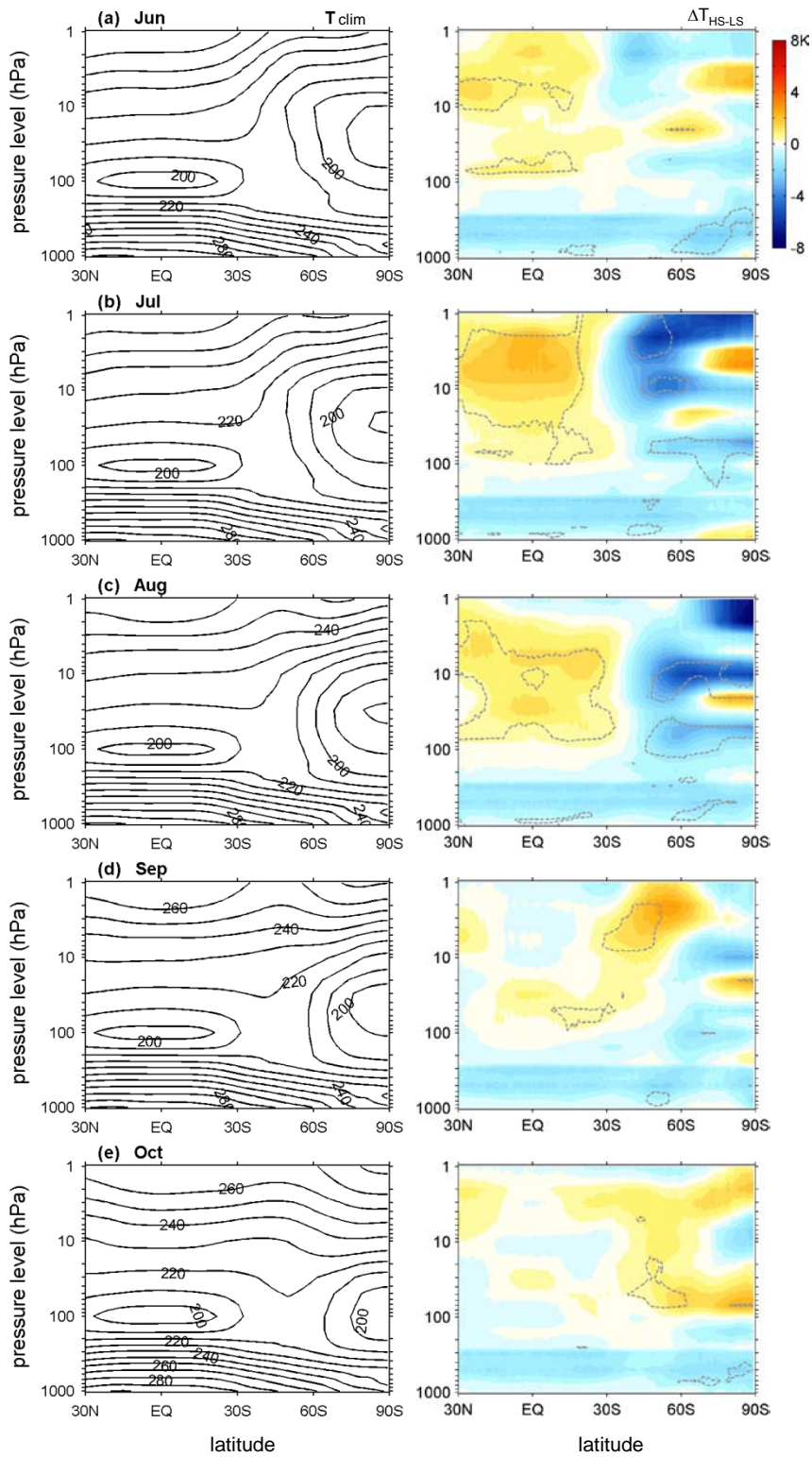


Figure 3

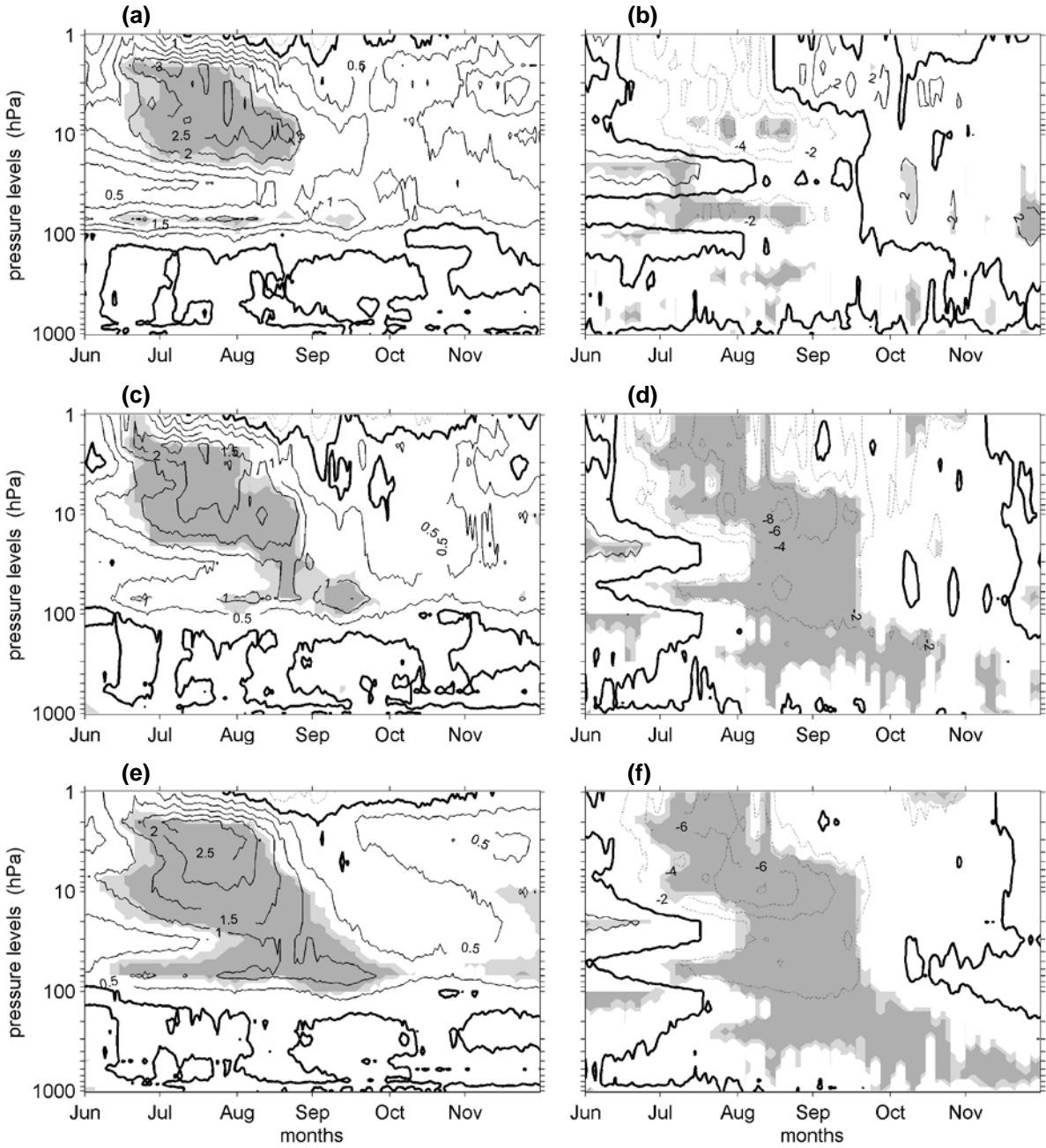


Figure 4

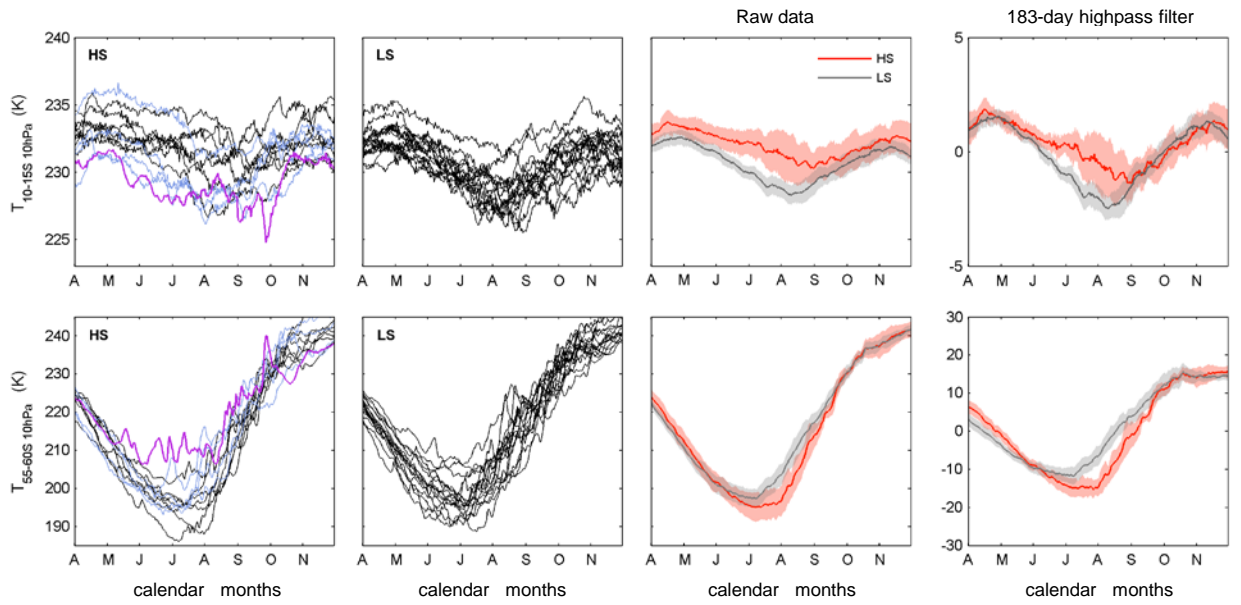


Figure 5

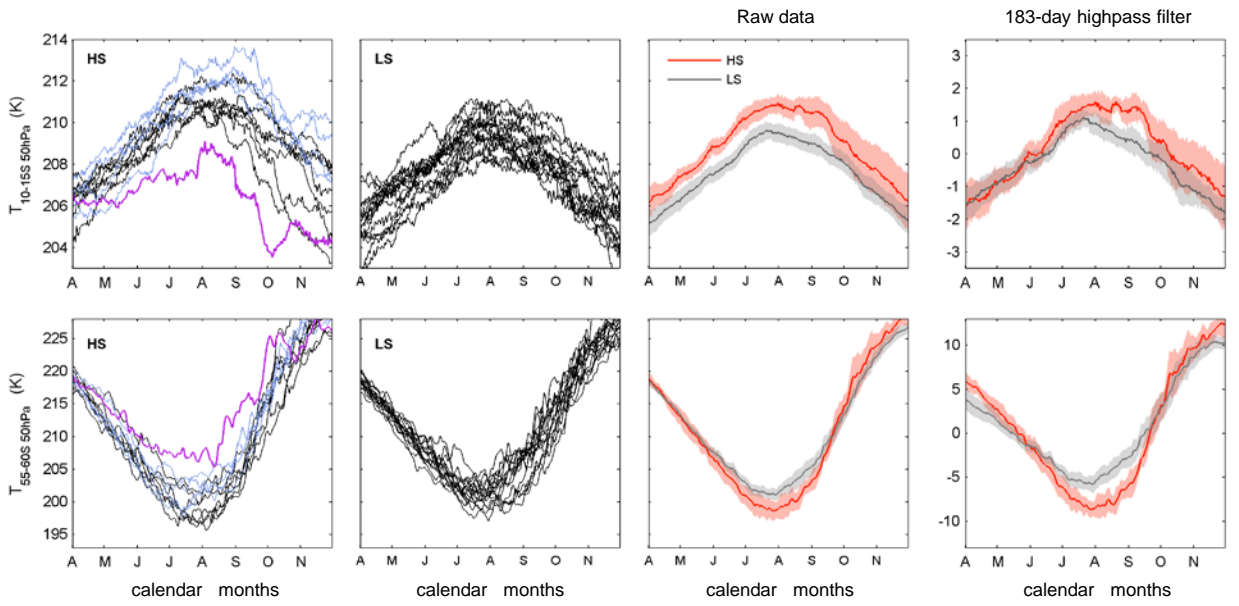


Figure 6

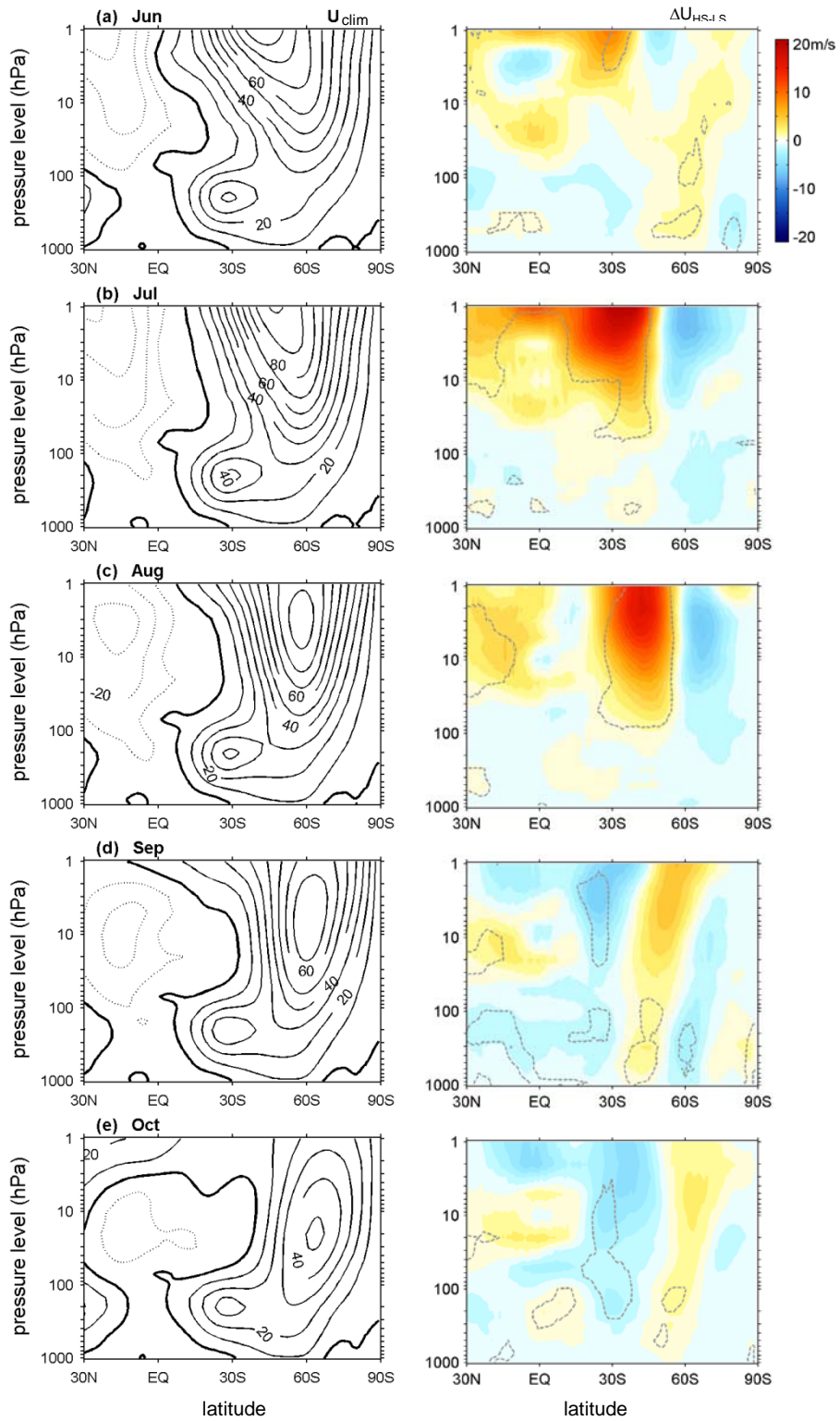


Figure 7

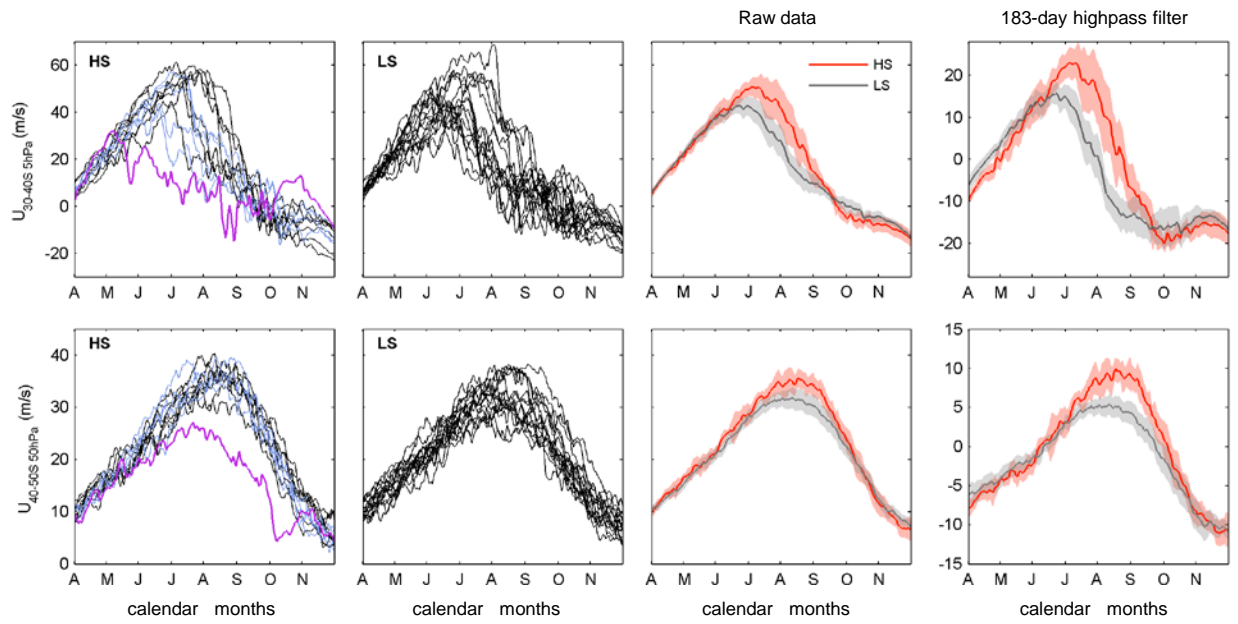


Figure 8

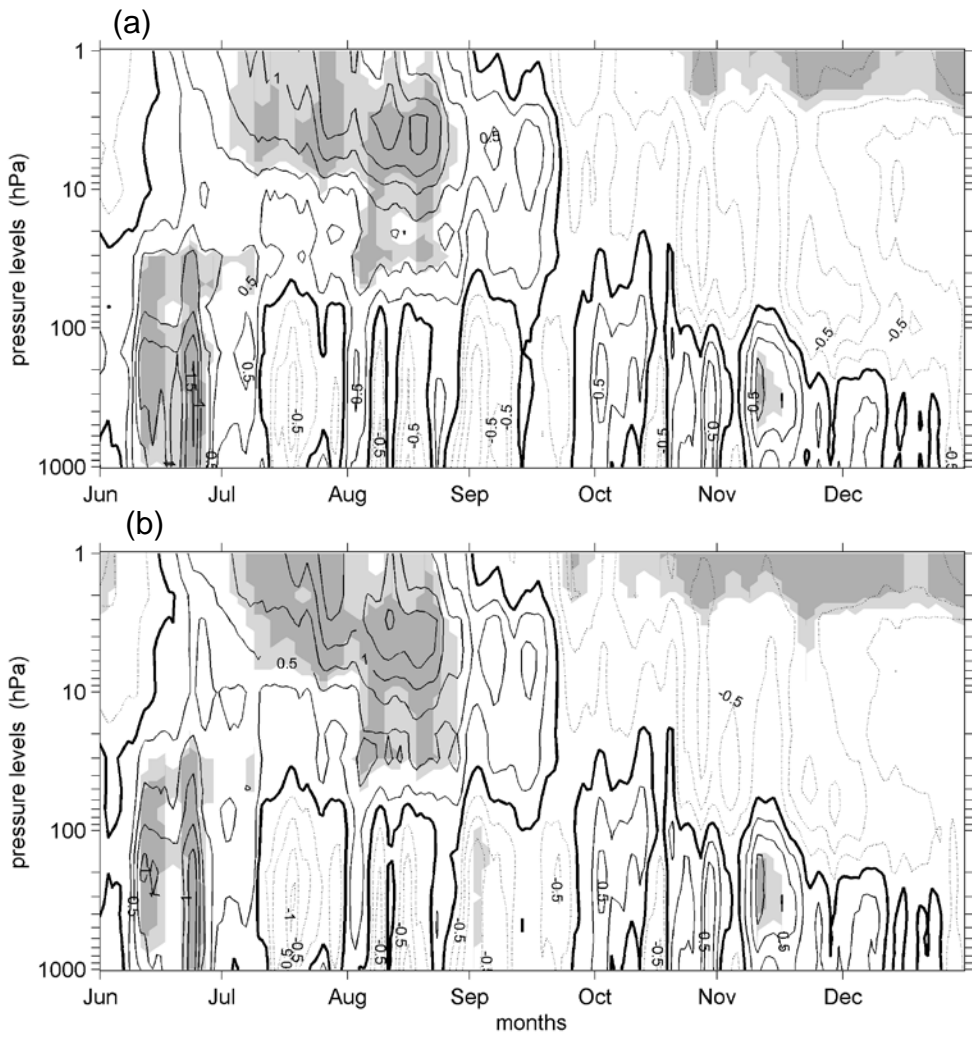


Figure 9

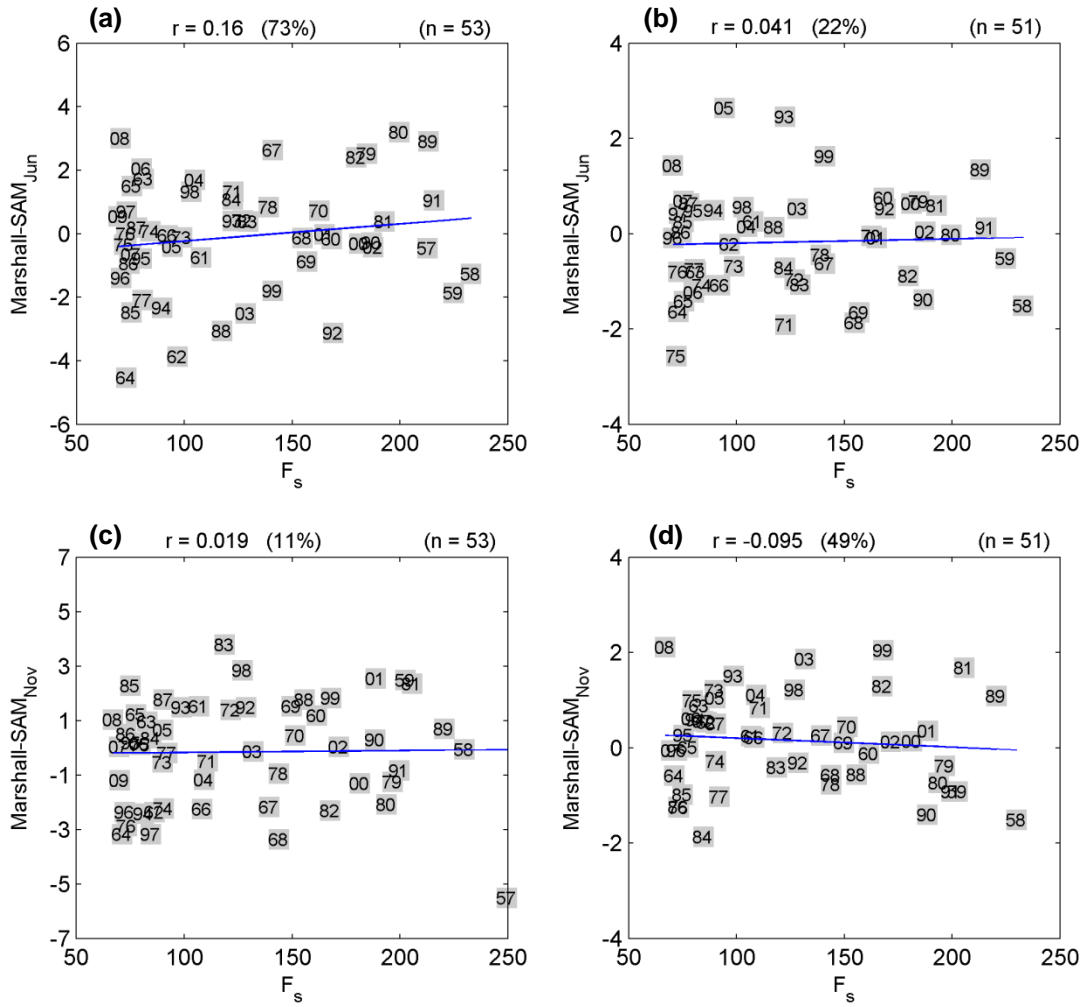


Figure 10